

# Permeability of Microcracked Solids with Random Crack Networks: Role of Connectivity and Opening Aperture

Le Li<sup>1</sup> · Kefei Li<sup>1</sup> 

Received: 16 November 2014 / Accepted: 13 May 2015 / Published online: 23 May 2015  
© Springer Science+Business Media Dordrecht 2015

**Abstract** This paper investigates the permeability of microcracked porous solids containing 2D random crack networks. The past works on permeability of crack networks are firstly reviewed. The geometry analysis is performed on numerical samples of crack networks with different crack length distributions, crack densities, domain size ratios and clustering degrees. The parameters from continuum percolation theory are used to characterize the geometry of random networks including the percolation threshold, the scaling exponents for percolation probability and correlation length of crack clusters, and the fractal dimension of spanning clusters. The crack density is used as the basic percolation variable, and a new connectivity factor is proposed for the cluster spanning in finite domain. Then the effective permeability of porous matrix containing 2D random crack networks is analyzed on numerical samples via finite element method. A scaling law for effective permeability is established near the percolation threshold taking into account the matrix permeability, crack opening aperture, crack connectivity and tortuosity. The results from geometry analysis and permeability analysis show that: (1) The new connectivity factor is proved pertinent to network percolation, related to both crack density and crack clustering degree; (2) the percolation parameters of uncorrelated crack networks are rather near to the universal values from the continuum percolation theory, but their values change with the clustering degree of crack networks; (3) the numerical results confirm the scaling law proposed for effective permeability, and the permeability is found to scale with the crack opening through a power law.

**Keywords** Permeability · Crack network · Percolation · Connectivity · Fractal dimension · Opening aperture

---

✉ Kefei Li  
likefei@tsinghua.edu.cn

<sup>1</sup> Key Laboratory of Structure Safety and Durability of China Education Ministry, Department of Civil Engineering, Tsinghua University, Beijing 100084, People's Republic of China

## 1 Introduction

Permeability of solids is a physical property valued by various engineering applications (Wong et al. 1984). For engineered materials, the permeability is closely related to its function and durability (Pan et al. 2010; Loosveldt et al. 2002). For multiphase porous solids, the permeability depends both on the properties of each phase and on the microstructure including volume fractions, spatial distribution and geometry of the phases (Torquato 1991). The presence of cracks, intrinsic or induced by external actions, can greatly facilitate the flow of fluids and thus alter the permeability of porous solids (Hearn 1999). For quasibrittle materials like concrete and rocks, the presence of cracks can further trigger the mass transport and exchange between the solid phases and external fluids, deteriorating the long-term durability of materials (Suzuki et al. 1998; Samaha and Hover 1992). Thus, mastering the impact of cracks on the permeability of porous solids is fundamental for various engineering applications.

Relationship between geometry characteristics of crack network in solids and the effective permeability has attracted great attention over the past decades; the connectivity, length, density, aperture and orientation of cracks are regarded as control parameters for the permeability of cracked porous solids (Lespinasse et al. 2005; Adler et al. 2013). From the point of view of effective medium theory (EMT), the cracks can be regarded as inclusions with large local permeability in a homogeneous porous matrix (Pouya and Ghabezloo 2010). The homogenization techniques from computational composite theory can help to solve the permeability of materials having homogeneously distributed cracks in statistical sense (Guéguen and Dienes 1989). Multiple schemes have been derived from EMT models: The dilute solution considers cracks to be isolated and embedded in homogeneous matrix with determined property (Kachanov 1992); the self-consistent approximation idealizes the cracked material as a single crack embedded in a matrix with properties of the effective medium (Berryman and Hoversten 2012); the differential scheme solves the permeability through an iterative procedure until the cracks attain the desired concentration (Norris 1985). The interaction direct derivative (IDD) scheme (Zheng and Du 2001), a simplified self-consistent scheme, provides a direct solution for permeability without iteration and has been applied to the solution of permeability of microcracked solids with low crack density (Zhou et al. 2011).

The fundamental idea of these EMT models is to treat the influence of cracks on fluid flow in a homogenized way, and these models fail as the local connectivity or clustering of cracks dominates the flow pattern (Li and Zhang 2011). In the latter case, the representative elementary volume (REV) loses its meaning for the cracked porous materials and the prediction of permeability is beyond the reach of EMT models. As the theoretical counterpart, the percolation theory provides concepts and methods to quantify the clustering of crack networks and the effect on the material properties like permeability (Guéguen et al. 1997). The classical percolation theory is based on lattice concepts and more adapted to solve the properties of materials with regular crack networks (Wilke et al. 1985), and some efforts have been taken to idealize the random networks to the equivalent lattices (Hestir and Long 1990; Leung and Zimmerman 2012). The continuum percolation theory, more recently developed, is more adapted to the materials with random or less regular crack networks (Somette 1988) and has been applied to the connectivity analysis of random fractures (Berkowitz 1995) and the permeability estimate of soils with discrete pore geometry (Berkowitz and Ewing 1998; Hunt and Ewing 2009). Albeit these developments, the results from percolation theory, continuum- or lattice-based, are far from enough to provide satisfactory prediction for permeability of

solids incorporating random crack networks, and the role of such crucial geometry factors as the connectivity and opening aperture are not yet included in the permeability prediction. A detailed review of the relevant results is given in Sect. 2.

In this paper, we attempt to characterize the geometry of random crack networks and then establish the relation between geometrical characterization of crack network and the material permeability through a continuum percolation approach. To this purpose, the past works on the relation between crack geometry and permeability are reviewed in Sect. 2; the geometry characteristics of random crack networks are studied in Sect. 3 for 2D cases, and a new connectivity factor is defined; the scaling law of permeability is established for microcracked porous media near percolation threshold considering the crack opening aperture in Sect. 4; and the concluding remarks are given in Sect. 5.

## 2 Permeability of Cracked Solids: Review

The most recent results on the relation between the geometry of cracks and the effective permeability are reviewed in the following from EMT models, percolation theory and numerical simulations. A recent EMT model dedicated to the permeability of cracked solids is due to Zhou et al. (2011). The model uses the IDD scheme and considers the cracks as inclusions into homogeneous porous matrix with infinite local permeability. Based on the dilute solution for penny-like crack inclusions (Shafiro and Kachanov 2000), the effective permeability of solids incorporating randomly distributed cracks in 2D case writes,

$$\frac{K}{K_m} = \frac{1 + \frac{\pi}{2}(1 - \gamma_D)\rho_2}{1 - \frac{\pi}{2}\gamma_D\rho_2} \tag{1}$$

where  $K$ ,  $K_m$  are, respectively, the permeability of cracked solid and homogeneous matrix,  $\rho_2$  is the area density of cracks, and  $\gamma_D$  is the shape function for the penny cracks. These results are extended to crack networks with finite connectivity by introducing an amplification factor to the crack density,

$$\rho'_2 = (1 + \beta'\phi)\rho_2 \tag{2}$$

where  $\beta'$  denotes the local amplification of fluid flow by crack connection, and  $\phi$  is the connectivity ratio of connected cracks with respect to total cracks. Through numerical simulation on numerical cells, the amplification factor  $\beta'$  is expressed in terms of crack density and connectivity ratio. This model takes into account the effect of finite connectivity of cracks on permeability, but no analytical result is obtained for the amplification factor  $\beta'$ , and this model will not be valid as the cracks are highly connected and form a percolation path for fluid flow.

Following percolation theory, Mourzenko et al. (2004) investigated the permeability of 3D crack networks containing plane polygons randomly oriented with a power law distribution for crack size:  $n(l) = \alpha l^{-a}$ , where  $n(l)dl$  is the number of cracks with radius in the range  $[l, l + dl]$  and  $\alpha$  a normalization coefficient. The macroscopic permeability  $K$  was proposed in a general expression as,

$$K = \rho\langle\sigma' A_p\rangle K'_2(\rho'_3) \tag{3}$$

Here the term  $\rho\langle\sigma' A_p\rangle$  represents the volumetric area of cracks, weighted by the individual crack permeability; the  $K'_2$  is a function of the dimensionless density  $\rho'_3$  that controls the network percolation, and incorporates the influence of the crack shape and size distributions.

The percolation threshold  $\rho'_{3c}(L')$  of crack networks depends on the geometry of cracks and can be expressed as,

$$\rho'_{3c} = \alpha_{3c} \left[ 1 - 4 \left( \eta' - \frac{2}{\pi} \right)^2 \right] \tag{4}$$

where  $\alpha_{3c} = 2.69$  for mesh size  $L' = 6$  and  $\alpha_{3c} = 2.41$  for  $L' \rightarrow \infty$ ;  $\eta'$  is a shape factor with  $\eta' = 2/\pi$  for disks. For infinitely elongated objects ( $\eta' \rightarrow 1$ ),  $\rho'_{3c}(\infty) = 1.14$ . Two heuristic analytical models were proposed from numerical simulations, i.e.,

$$\begin{cases} K'_2 = \frac{2}{3} \left[ 1 - \frac{1}{0.1(\rho'_3 + 6.6)} \right] & \text{for } \rho'_3 \gg \rho'_{3c} \\ K'_2 = \frac{0.1}{\rho'_3} (\rho'_3 - \rho'_{3c})^{1.6} & \text{for } \rho'_3 \sim \rho'_{3c} \end{cases} \tag{5}$$

No sharp change of  $K$  is predicted by the second equation as  $\rho'_3 \rightarrow \rho_{3c}$ , and the permeability of homogeneous matrix is assumed to zero.

Jafari and Babadagli (2013) proposed the effective permeability of rocks containing 2D fracture networks in terms of a percolation term,  $\rho' - \rho'_c$ , as

$$K = 88.411 (\rho' - \rho'_c)^{0.4602} \tag{6}$$

The 2D crack density  $\rho'$  is defined as  $\rho' = \frac{N}{L^2} A_{ex}$ , where  $N$  is the number of cracks in the domain  $L \times L$ , and  $A_{ex}$  is the excluded area of cracks. The authors used  $L = 100$  m and  $\rho'_c = 3.6$  taken as the continuum percolation threshold from Adler and Thovert (1999). The above model applied to  $\rho' > \rho'_c$  and the aperture of fracture were considered to be less influential for permeability compared to fracture density and length. Note that this assumption was reached for the fracture length attaining 80m, almost the domain size, and the influence of fracture aperture can be different for domains containing much shorter fractures and local crack clustering.

Yazdi et al. (2011) provided an expression for the effective permeability of 2D crack networks with finite crack aperture  $W$  for crack density  $\rho' = 1.59 \sim 89.52$ . The permeability  $K$  scales with the ratio  $b$ , ratio between the crack aperture  $W$  and crack length  $l$ , through a power law,

$$K \propto b^{-0.02\rho'+1.1} \tag{7}$$

where crack density  $\rho'$  has the same definition in Eq. (6). Since the corresponding percolation threshold  $\rho'_c$  was not provided for this analysis, the validity range of this scaling law cannot be located with respect to the percolation threshold. However, it is clear that the scaling law  $K - b$  depends also on the crack density  $\rho'_c$ .

de Dreuzy et al. (2001a) investigated the relationship between the permeability and the connectivity for random crack networks with power law length distribution, i.e.,  $n(l) = \alpha l^{-a}$ . It was showed that the exponent  $a$  governs the flow patterns: The flow by long fractures dominates for  $a < 2$ , the percolation controls the flow as  $a > 3$ , and a mixed pattern exists in between. Further, de Dreuzy et al. (2001b) investigated the influence of crack length (power distribution) and crack aperture (lognormal distribution) on the permeability of 2D crack networks  $K$  and found the following simplified law for correlated length and aperture of cracks,

$$\log K = \delta_M \bar{b} + \frac{\omega_M}{2} \bar{b}^2 \tag{8}$$

where  $\bar{b}$  is the standard deviation of the crack aperture, and  $\delta_M, \omega_M$  are geometry parameters of random networks depending on the length ratio between domain size and crack characteristic length, exponent  $a$ , and percolation parameter. In their later work (de Dreuzy et al.

2002), the crack length and aperture of both power distributions were investigated following the same framework.

From a purely numerical simulation scheme, [Leung and Zimmerman \(2012\)](#) proposed the following scaling law for the permeability (hydraulic conductivity)  $K$  of random 2D crack networks,

$$\frac{K}{K_R} = B\sqrt{1 + 2\zeta} \frac{n\bar{l}}{2L} \tag{9}$$

Here  $K_R$  is the reference hydraulic conductivity of domain  $L \times L$  containing orthogonal pair of cracks with uniform aperture,  $\zeta$  is the ratio between the node number of crack networks and total crack number  $n_{\text{node}}/n$ ,  $\bar{l}$  is the average of crack length, and  $B$  is the regressed constant taken as  $9.26 \times 10^{-2}$  in this study. This expression contains actually the information of crack connectivity through  $\zeta$ , and crack size and density through  $n\bar{l}/L$ . No explicit percolation was provided from this result. In the same literature, the influence of variation of fracture aperture was represented through a power average ([Desbarats 1992](#)),

$$\hat{K} = \left( \frac{1}{n} \sum_{i=1}^n K_i^\omega \right)^{1/\omega} \tag{10}$$

where  $K_i$  is the permeability (hydraulic conductivity) of fracture  $i$ ,  $\hat{K}$  is the equivalent permeability for all fractures, and  $\omega$  is the averaging power. Then permeability of 2D random crack networks with different apertures was estimated by  $K_{CB} = \hat{K}(1 - 2f')$  with  $f'$  for the ratio of non-conducting bonds. The authors found that the arithmetic average, i.e.,  $\omega = 1$ , gives the best estimation for effective permeability. [Bogdanov et al. \(2003\)](#) used direct numerical method to determine the permeability of porous media incorporating 3D random crack systems through the solution of steady single-phase flow equations in periodic porous unit cells. The effective permeability was showed to assume different expressions for low, intermediate, large and very large crack densities.

On the basis of the above results from EMT, percolation theory and numerical simulations, this paper aims to solve the permeability of microcracked solids incorporating random crack networks. The basic concepts and methods from continuum percolation theory are used to describe the geometry characteristics and to establish the scaling law. In the geometry characterization of random crack networks, the concept of fractal dimension is adopted, and the focus is on the pertinent definition of the connectivity of random crack networks. The scaling law of effective permeability is proposed through the connectivity and tortuosity of the crack networks, and the role of crack opening aperture is investigated particularly.

### 3 Geometry of Random Crack Networks

#### 3.1 Percolation Basis

Classical percolation theory uses lattice or bond model to illustrate the percolation concepts: The probability of a site or a bond being occupied is  $p$ , and the probability at which a percolating cluster occurs,  $p_c$ , is called the critical probability or percolation threshold. In other words, for  $p > p_c$ , at least one percolating cluster exists and no percolating cluster exists as  $p < p_c$ . As  $p \rightarrow p_c$ , the following scaling law holds,

$$P(p) \propto (p - p_c)^\beta, \quad \xi(p) \propto (p - p_c)^{-\nu} \tag{11}$$

where  $P$  is the probability that any site or bond belongs to the percolating cluster, and  $\xi$  is correlation length between the percolating clusters. The exponents  $\beta, \nu$  are universal constants in classical percolation theory, i.e.,  $\beta = 5/36$  and  $\nu = 4/3$  for 2D case according to [Stauffer and Aharony \(2003\)](#).

In a finite domain  $L \times L$ , the percolation threshold depends on the domain size, i.e.,  $p_c^L = p_c(L)$ . Normally this size-dependent threshold  $p_c^L$  is not a sharp function but repeating numerical simulations can help to determine the value ([Stauffer and Aharony 2003](#)). Moreover,  $p_c^L \rightarrow p_c$  as  $L \rightarrow \infty$ . Under this situation, the domain size appears in the scaling laws in Eq. (11) and writes,

$$P(L, p) \propto (p - p_c)^\beta h[(p - p_c)L^{1/\nu}], \quad \xi(L, p) \propto L(p - p_c)^{-\nu} h[(p - p_c)L^{1/\nu}] \tag{12}$$

with  $h$  as a nonsingular function, e.g., in Gaussian form ([Stauffer 1979](#)). This expression is of vital importance since it is supposed to apply to all the quantities associated with the percolation networks. For random crack networks in a finite domain, the above classical site/bond percolation theory is extended to continuum percolation theory, and the scaling law in Eq. (12) is assumed to still hold but adopt different scaling exponents ([Masih and King 2007](#); [Halperin et al. 1985](#)). The main difference between the classical and continuum percolations resides in the definition of probability  $p$ , that is, for random crack networks, the probability is substituted by the crack density  $\rho$ . For a random network with  $n$  cracks in a finite domain  $L \times L$ , the crack density is defined as,

$$\rho = \frac{1}{L^2} \sum_{i=1}^N \left(\frac{l_i}{2}\right)^2 \tag{13}$$

with  $l_i$  for the length of  $i$ th crack. Accordingly, the percolation threshold,  $\rho_c$ , is the crack density at which a percolating cluster appears in statistical sense. Certainly, this threshold depends on the geometry characteristics such as the domain size, crack length as well as crack orientation.

### 3.2 Fractal Dimension and Connectivity

The random crack clusters are assumed to have fractal properties ([Davy et al. 1990](#)). In this study, the fractal property of crack clusters is described by the two-point correlation function ([Darcel et al. 2003](#)), which describes the spatial correlation of the cracks. This correlation function depicts the probability of two cracks within a distance  $r$  belonging to the same cluster, defined as,

$$C(r) = \frac{N(r)}{N_T} \tag{14}$$

with  $N_T$  for the total crack center number of all cracks and  $N(r)$  the number of crack centers of which mutual distance is within  $r$ . The function  $C(r)$  is expected to scale with the distance  $r$  through a fractal dimension  $D_c$ ,

$$C(r) \propto r^{D_c} \tag{15}$$

and the fractal dimension  $D_c$  can be read from the linear regression  $C(r) \sim r$  on logarithm scale.

The connectivity is recognized as one crucial geometry parameter for fluid flow in random crack networks, and some straightforward definitions are available in the literature: the average number of intersections per crack ([Robinson 1984](#)), the density of the degree of freedom

(DDOF) (Li and Zhang 2011), or the ratio of connected cracks (Zhou et al. 2012). These definitions are all from average point of view, and local clustering of cracks is not taken into account. It will be showed later that local clustering, under the same average connectivity, can change the flow substantially. To improve the definition, a new connectivity factor,  $f$ , is defined for domain  $L \times L$  considering the local clustering effect through the fractal dimension of crack clusters,

$$f = \frac{\xi}{L} [P(\rho, L)]^{(3-D_c)}, \quad \text{with } f \in [0, 1] \tag{16}$$

where  $\xi$  is correlation length of clusters or the cluster size, and  $P(\rho, L)$  is the likelihood of a crack being connected to the spanning clusters. The term  $P(\rho, L)$  can be determined as the area ratio between the spanning cluster and the whole network. This definition includes both the cluster size  $\xi$  and the local clustering effect through  $D_c$ . Note that  $f \rightarrow 1$  as  $P \rightarrow 1$  (all cracks belong to one spanning cluster) and  $L \rightarrow \xi$ . Using the scaling law in Eq. (12), the connectivity  $f$  around percolation threshold adopts the scaling law

$$f \propto |\rho - \rho_c|^{-\nu+(3-D_c)\beta} \tag{17}$$

### 3.3 Numerical Generation of Random Crack Networks

A numerical repeating unit cell (RUC) is established for the finite domain  $L \times L$ . The statistical properties are attributed to the crack length and opening apertures. This study adopts lognormal distribution for crack length following the geometrical analysis on cracks of concrete specimens after axial loading in Zhou et al. (2012), cf. Fig. 1. The probability density function of crack length is,

$$g(l; \delta, \sigma) = \frac{1}{l\sigma\sqrt{2\pi}} e^{-(\ln l - \delta)^2 / 2\sigma^2} \quad (l > 0) \tag{18}$$

where  $\delta$  and  $\sigma$  are the mean value and variance of logarithm crack length.

The statistical analysis revealed that the crack opening aperture is well correlated to the crack length (Zhou et al. 2012). Accordingly, the ratio of opening aperture to length,  $b$ , is

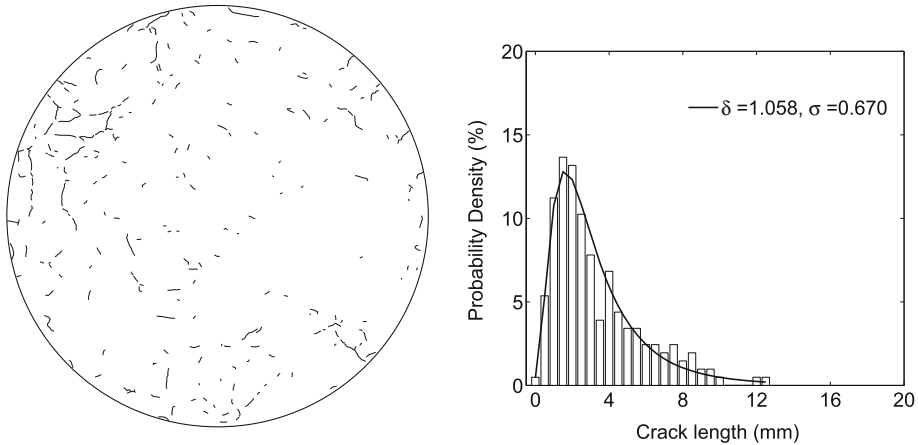


**Fig. 1** Crack network (left) and crack length distribution (right) for Specimen OPC7-2 after uniaxial loading in Zhou et al. (2012)

**Table 1** Crack patterns retained for geometry and permeability simulations

Analysis	Crack length distribution	Domain size $x = L/l_{\text{mean}}$	Density $\rho$	Fractal dimension $D_c$	Aperture ratio $b$
Geometry	Constant	$5 \sim 20 (\rho_c)$	$0, 3.0; 0.05 (\rho_c)$	$2.0 \sim 1.62 (\rho_c)$	–
		$3 \sim 50 (\beta, \nu)$	$0, \rho_c; 0.05 (\beta, \nu)$	$2.0 \sim 1.51 (\beta, \nu)$	–
	Lognormal	$10 \sim 30 (\rho_c)$	$0, 3.0; 0.05 (\rho_c)$	$2.0 (\rho_c)$	–
		$3 \sim 50 (\beta, \nu)$	$0, \rho_c; 0.05 (\beta, \nu)$	$2.0 (\beta, \nu)$	–
Permeability	Constant	30	$0, \rho_c; 0.05$	$2.0, 1.75, 1.62$	$0.001 \sim 0.028$
	Lognormal	30	$0, \rho_c; 0.05$	2.0	$0.001 \sim 0.028$

retained as a basic variable: The ratio is taken as  $0.001 \sim 0.028$  from the results in Zhou et al. (2012), corresponding to the absolute values of opening aperture equal to  $5 \sim 100 \mu\text{m}$  and  $l$  equal to 3.606 mm. In parallel, the case of constant crack length distribution is kept in geometry and permeability analysis for comparison purpose. So, the lognormal distribution of crack length has the mean length  $l_{\text{mean}} = 3.606 \text{ mm}$  and the standard deviation  $SD(l) = 2.716 \text{ mm}$ , and the constant distribution has the mean length  $l_{\text{mean}} = 3.606 \text{ mm}$ . A length scale  $x$  is defined as the ratio between the domain size  $L$  and the crack mean length  $l_{\text{mean}}$ . The ranges of parameters for the numerical simulation cases in this study are summarized in Table 1.

The numerical generation of a random crack network is realized through Monte Carlo algorithm as follows. The crack density  $\rho$  and the crack length distribution are first determined for the random crack network. The fractal dimension of crack networks  $D_c$  is controlled by the average number of interaction per crack,  $n_{\text{inter}}/N_T$  with  $n_{\text{inter}}, N_T$  standing, respectively, for the intersection number of cracks and total crack number. Then, cracks are generated, obeying the predetermined statistical distribution, and located randomly one by one into the domain  $L \times L$ . As one crack is positioned and the number of its intersection with the already generated cracks is calculated, this crack will be accepted if the intersection ratio on this stage does not exceed the expected value, otherwise the crack will be rejected. If the generated crack overlaps the domain boundary, its outer part is trimmed off. At the same time, the intersection ratio on this stage is calculated and checked, and the groups of isolated and connected cracks are updated. This procedure is repeated until the target density and intersection ratio are achieved. The generated crack network is subject to geometry analysis for crack clusters and the relevant percolation parameters, including the connectivity factor  $f$ . Releasing the control of the intersection ratio  $n_{\text{inter}}/N_T$  produces an uncorrelated network with cracks totally randomly distributed. Figure 2 illustrates an uncorrelated network and a network with intersection ratio of 3.0 for a same crack density ( $\rho = 0.75$ ).

Since the fractal dimension  $D_c$  and the connectivity factor  $f_c$  are controlled actually by the parameter  $n_{\text{inter}}/N_T$  in numerical simulations, it deserves to gain an insight on the impact of  $n_{\text{inter}}/N_T$  on the network geometry. To this purpose, Fig. 3 illustrates the random networks generated for a density  $\rho = 1.5$  but with  $n_{\text{inter}}/N_T = 0 \sim 5$ . The length ratio is fixed as  $x = 20$  and  $x = 30$  for constant and lognormal length distributions, and the fractal dimension  $D_c$  is evaluated through Eq. (15) as shown in Fig. 4a for constant crack networks. One can see that  $D_c$  decreases constantly with  $n_{\text{inter}}/N_T$ , and higher  $n_{\text{inter}}/N_T$  induces more important local clustering, so lower  $D_c$  means stronger local clustering. Thus both  $D_c$  and  $n_{\text{inter}}/N_T$  are related directly to local clustering degree of crack networks. But high local clustering will not necessarily contribute to the global connectivity; this point will be discussed further in



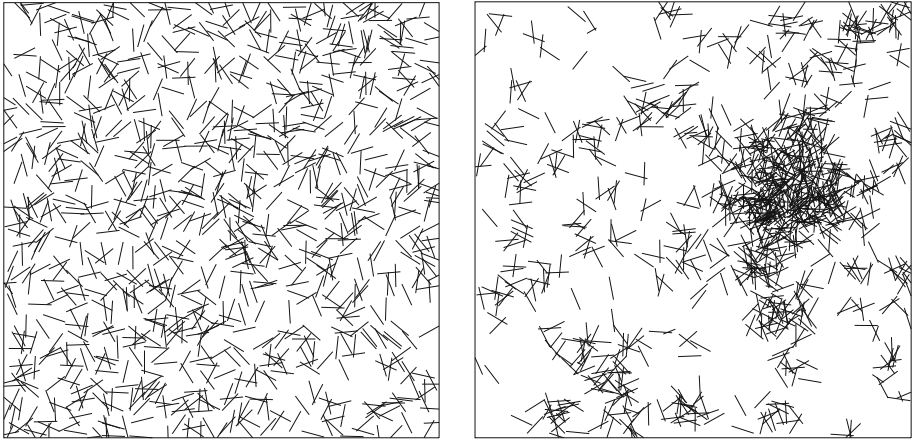


**Fig. 2** Crack networks with constant length,  $\rho = 0.75$ ,  $x = 20$ : uncorrelated network (left) and correlated network with  $n_{inter}/N_T = 3.0$  (right)

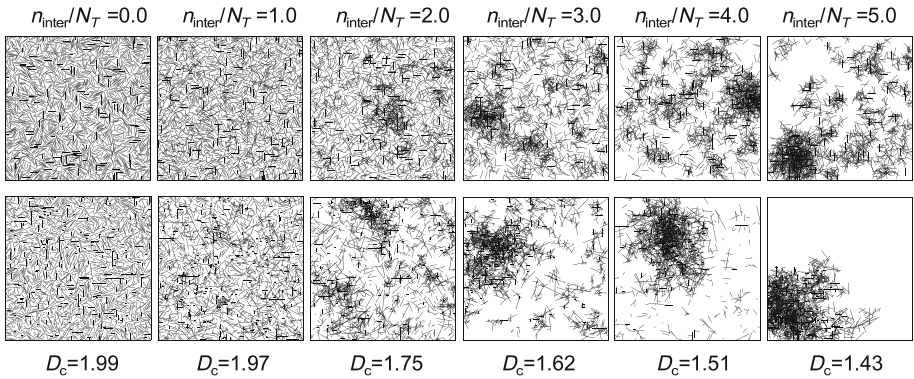


**Fig. 3** Examples of simulated crack networks with different  $D_c$  and different length distribution. From left to right, the fractal dimension decreases by improving the clustering: constant length distribution (up  $x = 20$ ); lognormal length distribution (down  $x = 30$ )

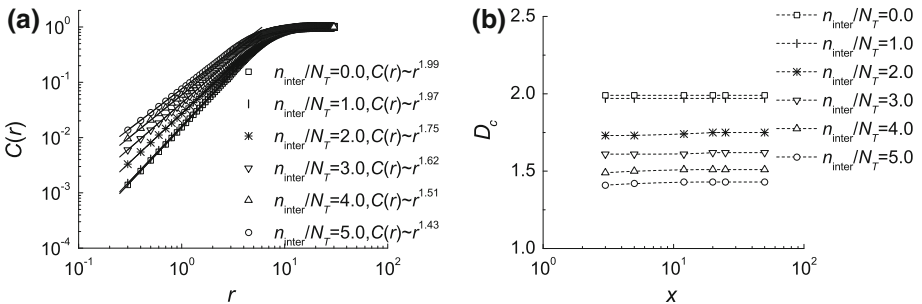


**Fig. 4** Regression of fractal dimension  $D_c$  in terms of  $n_{inter}/N_T$  through two-point correlation function (a) and in terms of length ratio  $x$  (b)

the geometry analysis part. The regression of the fractal dimension  $D_c$  is illustrated in Fig. 4a for different intersection ratios and in Fig. 4b for different length ratios. The  $D_c$  values are confirmed to relate closely with the  $n_{\text{inter}}/N_T$  ratio, and  $D_c$  remains nearly constant for large range of length ratio  $x$ . This indicates that the nature of fractal dimension  $D_c$  is not empirical but belongs to the intrinsic properties of the random crack networks.

### 3.4 Geometry Analysis of Random Crack Networks

**Percolation threshold  $\rho_c$**  The percolation threshold in terms of crack density  $\rho_c$  is obtained from Monte Carlo generation of random crack networks with predetermined crack length distribution and fractal dimension  $D_c$ . For a given domain size  $L$ , the crack networks are generated for density increasing from zero to 3.0, and for different length ratios  $x = L/l_{\text{mean}}$ , cf. Table 1. For each case (given  $\rho$  and  $x$ ), 400 random networks are generated, and the percolation probability is evaluated as the ratio of percolation networks with respect to total networks (400). Figure 5 shows the percolation thresholds for networks with different fractal dimensions and crack length distributions. For each simulation case, the point at which different probability curves intersect can be regarded as the percolation threshold. For the uncorrelated networks,  $D_c = 2.0$ , the thresholds  $\rho_c$  are, respectively, 1.43 and 1.67 for constant and lognormal length distributions. For correlated networks,  $\rho_c = 1.68$  for constant length with  $D_c = 1.75$  and  $\rho_c = 1.78$  for lognormal distribution with  $D_c = 1.62$ . Thus, the crack length distribution has impact on percolation threshold, and the thresholds are lower for uncorrelated networks for a same distribution. Note that the percolation threshold was evaluated as 5.6 for the dimensionless density  $\rho' = N_T l^2 / L^2$  in Bour and Davy (1997). This result can be converted to the crack density defined in Eq. (13) and is very near to the threshold for uncorrelated networks with constant cracks, i.e.,  $\rho_c = N_T l^2 / 4L^2 = 1.43$ .

**Exponent  $\nu$  and  $\beta$**  The exponent  $\nu$  is defined in Eq. (11) in the scaling law for correlation length  $\xi$ , which can be regarded as the mean cluster size near percolation threshold (Stauffer and Aharony 2003). The term  $\xi$  diverges as  $\rho \rightarrow \rho_c$  in infinite domain, while this exponent can be determined from the relationship  $\rho_c(x) - \rho_c \propto x^{-1/\nu}$  for finite domain (Stauffer and Aharony 2003). Given crack length distribution, fractal dimension  $D_c$  and length ratio  $x$ , random crack networks are generated with increasing crack density until percolation occurs in the finite domain, and the corresponding density is noted as a realized value for  $\rho_c(x)$ . Then this procedure is repeated for 400 simulations, and the average of these realized values is retained for  $\rho_c(x)$ . Since the  $\rho_c$  values are not known *a priori* for all the  $D_c$  cases, the standard deviation of  $\rho_c(x)$ ,  $\Delta\rho_c(x)$ , can be used instead of  $|\rho_c(x) - \rho_c|$  in the regression according to Stauffer and Aharony (2003). Thus the exponent  $\nu$  is to be regressed from  $\Delta\rho_c(x) \propto x^{-1/\nu}$  with  $\Delta^2\rho_c(x) = \langle\rho_c^2(x)\rangle - \langle\rho_c(x)\rangle^2$ .

Figure 6 illustrates the results for exponent  $\nu$  for two length distributions and different fractal dimensions. For networks of constant length, the exponent is obtained as  $1/\nu = 0.231 \sim 0.74$  for  $D_c = 1.51 \sim 2.0$ . Thus this exponent for correlation length is rather sensitive to the fractal dimension of networks. For comparison, the exponent of lognormal length for uncorrelated networks,  $D_c = 2.0$ , is evaluated as 0.73, rather near to the value of constant length of  $D_c = 2.0$ . Both values are close to the expected value  $3/4$  (Stauffer and Aharony 2003). Recent results show that, for crack length of power distribution, a similar exponent was obtained as  $|\rho_c(x) - \rho_c| \propto x^{-0.75}$  for crack length with power distribution (Sadeghnejad et al. 2013). It seems to confirm that this exponent is not sensitive to crack length distribution for uncorrelated networks but sensitive to the fractal dimension of correlated networks.

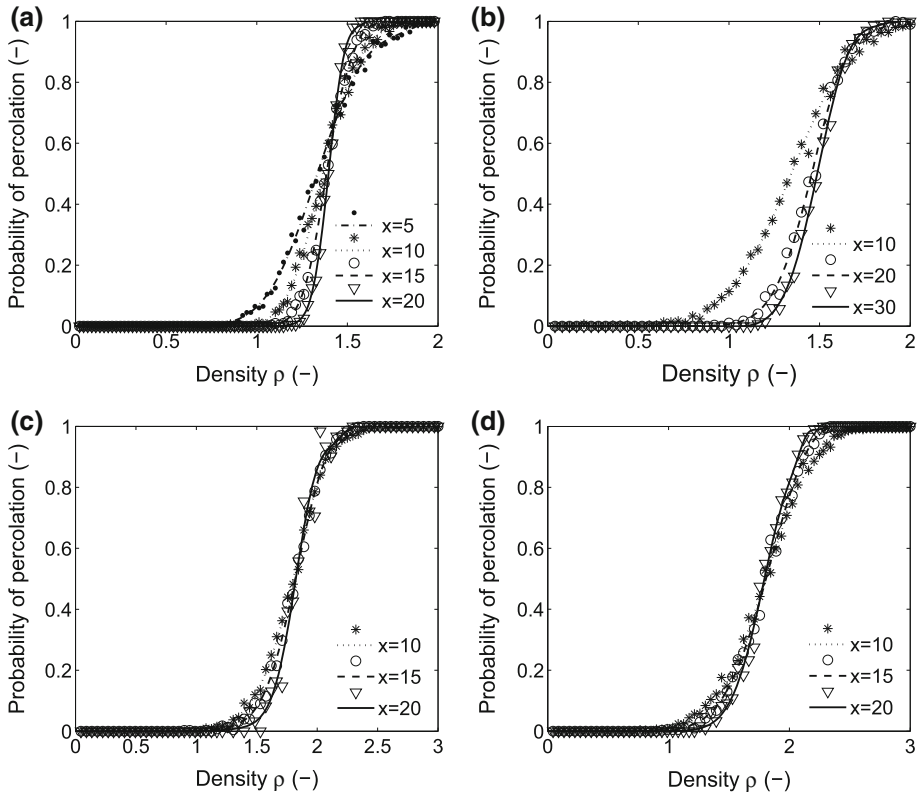


**Fig. 5** Percolation probability for finite-size domains: **a** constant length,  $D_c = 2.0$ , length ratio  $x = 5, 10, 15, 20$ ; **b** lognormal length,  $D_c = 2.0$ , length ratio  $x = 10, 20, 30$ ; **c** constant length,  $D_c = 1.75$ , length ratio  $x = 10, 15, 20$ ; **d** constant length,  $D_c = 1.62$ , length ratio  $x = 10, 15, 20$

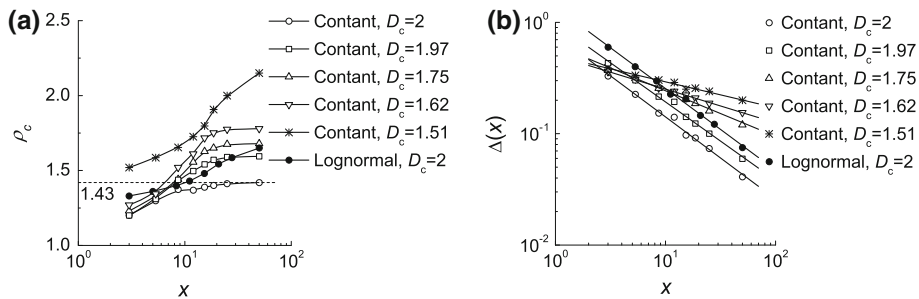


**Fig. 6** Exponent  $\nu$  from numerical simulations: **a** percolation density  $\rho_c(x)$  in terms of length ratio  $x$ ; **b** deviation  $\Delta\rho_c(x)$  in terms of length ratio on logarithm scale

Substituting the relationship  $\rho_c(x) - \rho_c \propto x^{-1/\nu}$  into Eq. (12), one can get  $P \propto x^{-\beta/\nu}$ . Here the term  $P$  should be interpreted as the ratio between the accumulated area of cracks in the spanning cluster  $A_b$  and the whole area of network  $A_N$ . Based on the same simulation results in Fig. 6, the regression of exponent  $\beta$  is given in Fig. 7a for both constant and lognormal distributions. For constant length, the term  $\beta/\nu$  ranges from 0.232 to 0.106 for

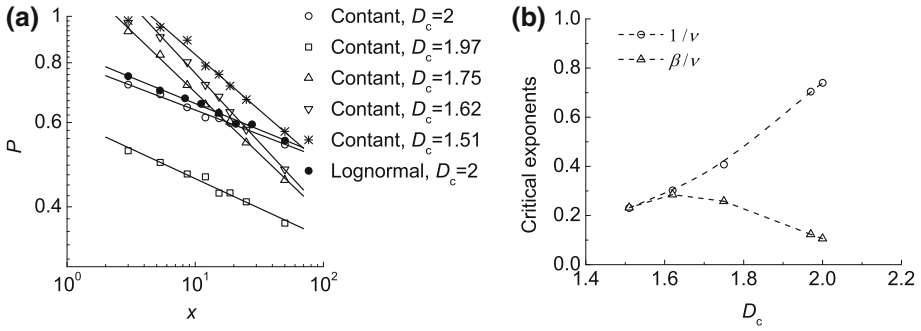


**Fig. 7** Exponent  $\beta$  for random crack networks: **a** regression of  $1/\beta$  through  $P \sim x$  relation for different  $D_c$ ; **b** exponents  $1/\nu, 1/\beta$  in terms of  $D_c$

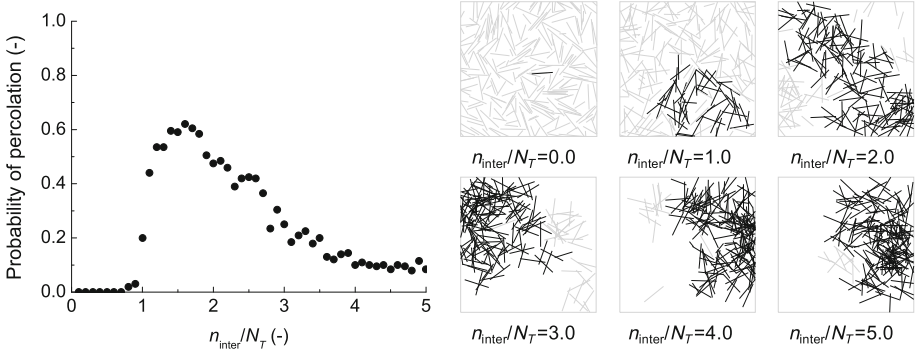


**Fig. 8** Percolation probability in terms of intersection ratio ( $n_{inter}/N_T = 0 \sim 5$ ) for constant length distribution, length ratio  $x = 5$  and crack density  $\rho = 1.5$ . The maximum crack clusters are highlighted

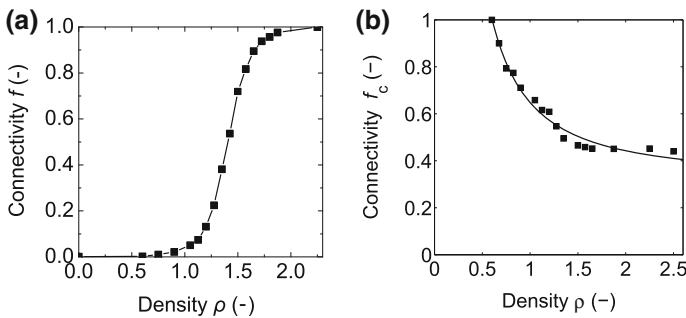
$D_c = 1.51 \sim 2.0$ . For uncorrelated networks, the difference of  $\beta/\nu$  between constant and lognormal lengths is quite small. Again, it seems that  $\beta/\nu$  is quite sensitive to  $D_c$  and remains constant for uncorrelated networks. For constant length, the variation of  $1/\nu$  and  $1/\beta$  is given in Fig. 7b, showing both exponents are fractal dependent.

**Connectivity factor  $f_c$**  The connectivity of crack networks is closely related to the pre-determined  $n_{inter}/N_T$  and the resulted fractal dimension  $D_c$ . To deepen this relation, Fig. 8 illustrates the probability of percolation for the random networks for  $n_{inter}/N_T = 0 \sim 5$ , the crack density  $\rho = 1.5$ , length ratio  $x = 5$  and constant crack length. Each probability of percolation is the ratio of percolated networks with respect to 400 random simulations. In the figure are also extracted six numerical samples for each  $n_{inter}/N_T$  ratio, and the connected cracks in the maximum cluster are highlighted compared to the isolated cracks. One can see clearly that the intersection ratio contributes to network percolation as  $n_{inter}/N_T \sim 1.5$  and the percolation probability decreases as the ratio increases further. From the numerical samples, high intersection ratios induce strong local clustering but decrease the global connectivity, in other words, high intersection ratio creates dense but local clusters in crack networks. This adverse effect of intersection ratio on network percolation has never been reported. The geometry parameters evaluated from Fig. 8 are given in Table 2.

Figure 9a illustrates the connectivity factor in terms of the crack density for constant crack length and  $D_c = 2.0$ . Each  $f$  value corresponds to the average of 400 numerical samples. One can see that  $f \sim \rho$  relation is similar to the percolation probability in terms of  $\rho$  in

**Table 2** Cluster and connectivity analysis for crack networks with different intersection ratios

$n_{inter}/N_T$	Total cracks	Isolated cracks	Maximum cluster size	Average cluster size	Fractal dimension $D_c$	Connectivity $f$
0	246	246	1	1	1.99	0.001
1	213	29	55	19	1.97	0.180
2	204	11	161	51	1.75	0.676
3	218	1	187	44	1.62	0.479
4	213	2	199	71	1.51	0.501
5	212	0	203	106	1.43	0.473



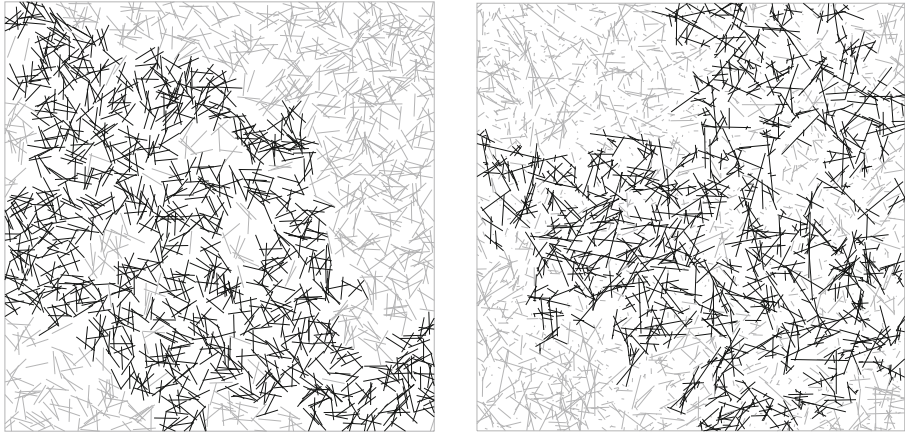
**Fig. 9** Connectivity analysis of networks with constant length cracks and length ratio  $x = 20$ : **a** connectivity factor in terms of crack density, **b** connectivity factor at percolation  $f_c$  in terms of crack density

Fig. 5:  $f$  increases gradually with  $\rho$  from 0 to 1. Note that the definition of  $f$  in Eq. (16) stipulates two conditions for  $f = 1$ : A spanning cluster occurs ( $\xi = L$ ) and all cracks belong to the spanning cluster ( $P(\rho, L) = 1$ ). So for most simulations  $f < 1$  even as the percolation occurs. This observation implies that the isolated cracks are also considered into the connectivity factor  $f$  as this factor is used in the permeability scaling law later in this paper. Figure 9b provides the connectivity factor at percolation  $f_c$  in terms of crack density  $\rho$ . The  $f_c$  is solved for a fixed density by increasing the  $n_{inter}/N_T$  ratio from 0 to 5 and using 0.1 as numerical increment, among these cases the minimum  $f$  value of all percolated cases is noted, and then this procedure is repeated for 200 times and the average of the minimum  $f$  values at percolation is noted for  $f_c$  at this density. The  $f_c \sim \rho$  curve in Fig. 9b should be interpreted with statistical sense: For the pair  $(f, \rho)$  below the curve, the occurrence of percolation is statistically low, while for the  $(f, \rho)$  pairs above the curve, the possibility of percolation is statistically high. The general idea of this curve is that the more is the crack density the less is the connectivity needed to reach percolation.

## 4 Permeability of random crack network

### 4.1 Scaling law for permeability

The permeability of solids incorporating crack networks relates to two groups of fundamental variables: the first to the permeability of the homogeneous matrix of (porous) solids  $K_m$  and the second to the characteristics of crack networks including the crack connectivity  $f$ , the



**Fig. 10** Examples of crack network and its backbone cluster at percolation: constant length distribution (*left*  $x = 20$ ,  $\rho = 1.43$ ,  $D_c = 2.0$ ); lognormal length distribution (*right*  $x = 30$ ,  $\rho = 1.67$ ,  $D_c = 2.0$ )

tortuosity  $\tau$ , the crack density  $\rho$  and the crack opening aperture  $b$ , i.e.,

$$K = K(K_m; f, \tau, \rho, b) \tag{19}$$

Among these parameters, the tortuosity  $\tau$  should be defined for the random crack network. In this study, the tortuosity is related to the dominating cluster (or “backbone” cluster), cf. Fig. 10. Note  $L_\xi$  the cumulative crack length in the backbone cluster and  $L_s$  its straight line length. The tortuosity is defined as the ratio  $\tau = L_\xi/L_s$  and  $\tau > 1$ . Assuming that the backbone cluster has fractal properties, the length  $L_\xi$  can be related to the measurement increment  $\epsilon$  though a fractal dimension  $D_\tau$  (Mandelbrot 1983),

$$L_\xi(\epsilon) = L_s \epsilon^{1-D_\tau} \tag{20}$$

Here  $D_\tau$  can assume the fractal dimension for the most probable flow path  $D_{opt}$  or the fractal dimension for the most probable traveling time  $D_b$  (Lee et al. 1999). These two values were quantified for spanning cluster of 2D random networks as  $D_{opt} = 1.21$  and  $D_b = 1.643$  in the literature (Sheppard et al. 1999). As the choice of  $\epsilon$  is arbitrary, letting  $\epsilon = (\xi/L)^{-1}$  gives,

$$L_\xi \left( (\xi/L)^{-1} \right) = L_s (\xi/L)^{D_\tau-1} \propto L_s (|\rho - \rho_c|^{-\nu})^{D_\tau-1} \tag{21}$$

Substituting this expression into the definition of tortuosity gives,

$$\tau = \frac{L_\xi}{L_s} \propto |\rho - \rho_c|^{\nu(1-D_\tau)} \tag{22}$$

With this definition, the conceptual scaling law in Eq. (19) can be put into the following form,

$$K = K_0(K_m, b) |\rho - \rho_c|^\mu \quad \text{with} \quad \mu = (3 - D_c)\beta - (2 - D_\tau)\nu \tag{23}$$

In this scaling law, the permeability is assumed to be linearly proportional to the connectivity factor  $f$  and inversely proportional to the tortuosity  $\tau$ , and thus the exponent  $\mu$  includes the connectivity in Eq. (17) and the tortuosity in Eq. (22), and the contribution of crack opening aperture and matrix permeability is included into the term  $K_0$ . Note that this scaling law applies only to the range  $\rho \rightarrow \rho_c$  due to the valid range of Eqs. (17) and (22). Physically the term  $K_0$  corresponds to the effective permeability as  $\tau, f \rightarrow 1$ , i.e., all the cracks form

**Table 3** Permeability scaling exponent  $\mu$ 

Crack length	$D_c$	$\rho_c$	$\beta$	$\nu$	Predicted $\mu$	Regressed $\mu$
Constant	2.0	1.43	0.143	1.351	-0.924	-0.922
Constant	1.97	—	0.175	1.420	-0.942	—
Constant	1.75	1.68	0.632	2.451	-1.146	-1.122
Constant	1.62	1.78	0.941	3.300	-1.308	-1.257
Constant	1.51	—	1.004	4.329	-1.924	—
Lognormal	2.0	1.67	0.147	1.368	-0.934	-0.919

a straight line and span across the finite domain  $L \times L$ . From this point of view, the  $K_0$  is supposed to scale to the square of crack opening, which will be re-discussed with numerical results. Adopting the most probable flow path fractal for  $D_\tau$ ,  $D_\tau = D_{\text{opt}} = 1.21$ , the scaling exponent  $\mu$  of permeability is evaluated in Table 3 as “predicted  $\mu$ ” for the simulation cases of geometry analysis in the previous section.

## 4.2 Numerical Analysis for Permeability

The permeability of solids incorporating random crack networks is solved through finite element methods (FEM). The numerical samples retained for permeability analysis are given in Table 1, and all cracks are idealized as 2-node elements and the matrix is discretized into 6-node triangle elements. All endpoints and intersection points of cracks are treated as common nodes between the 2-node and 6-node elements. The matrix takes the conventional intrinsic permeability for concretes, i.e.,  $K_m = 10^{-17} \text{m}^2$ . Note that a crack with opening of  $5 \mu\text{m}$  has the local permeability in the order  $10^{-11} \text{m}^2$ , 6 magnitudes higher than the matrix. The fluid is assumed incompressible and Newtonian and the flow observes the Navier–Stokes equation with small Reynolds number. With these assumptions, the effective permeability of the numerical samples can be evaluated between the flow rate  $q$  and the pressure gradient  $\nabla p$  through Darcy’s law  $q = -\nabla p \times K/\eta$  with  $\eta$  the fluid viscosity. In the numerical solution, the two opposite sides of numerical samples (cells) are treated as null flux condition and a pressure gradient is imposed on the other two opposite sides of samples.

To illustrate the effective permeability in terms of the crack density, Fig. 11 provides the effective permeability of uncorrelated crack networks for constant length distribution with  $D_c = 2.0$  and  $\rho_c = 1.43$ . One can see that at low crack density  $\rho \ll \rho_c$ , no percolation occurs and the effective permeability remains very low  $K/K_m \sim 1$ . As  $\rho \rightarrow \rho_c$ , the effective permeability increases substantially. The results confirm the determinant impact of crack percolation on the effective permeability. On the same figure is also illustrated the dispersion of permeability of the same random crack networks: A total of 40 simulations are performed for each density from 0 to 1.43 with increment of 0.05. The coefficient of variation ranges from 0.5% ( $\rho = 0.05$ ) to 19% ( $\rho = 1.4$ ), showing that larger dispersion is associated with higher crack density.

## 4.3 Permeability Scaling Exponent $\mu$

The effective permeability is solved for four cases: constant length with three  $D_c$  and log-normal length with  $D_c = 2.0$ , cf. Table 1. Since the purpose of this section is to regress the exponent  $\mu$ , the crack opening aperture is fixed at  $b = 0.013$  and the length ratio at

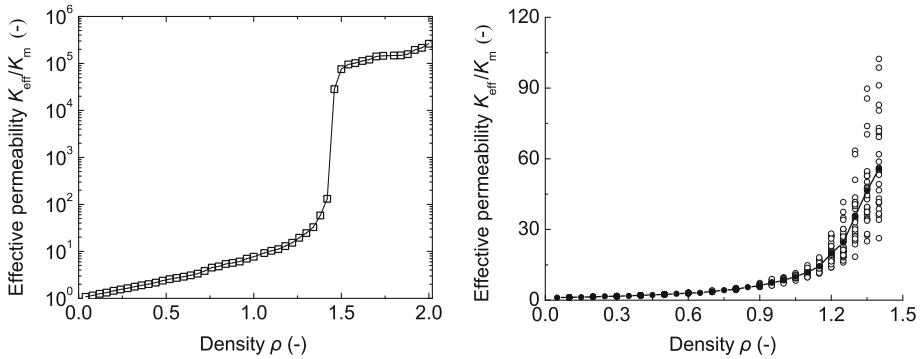


**Fig. 11** Effective permeability  $K_{\text{eff}}/K_m$  in terms of crack density for  $x = 30$ ,  $D_c = 2.0$  and constant length: percolation effect (left) and permeability dispersion (right)

$x = 30$ . In the regression of the exponent  $\mu$ , the crack density of networks changes from 0 to  $\rho_c$  by increment of 0.05 for each case, and for each density, 40 simulations are performed and average value is retained for the effective permeability. A total of 5160 simulations are performed for the regression of exponent  $\mu$ , and for each crack density  $\rho$ , the exponent  $\mu$  is read as the slope of  $\log K/K_m \sim \log|\rho - \rho_c|$  plot. Further, the valid range of the proposed scaling law in Eq. (23) is investigated following the plateau analysis on the  $\mu \sim \log|\rho - \rho_c|$  plot (Bonnet et al. 2001). Figure 12 gives the scaling exponent  $\mu$  in terms of  $|\rho - \rho_c|$  in logarithm scale. The valid range of the scaling law is well indicated by the lower cutoffs of plateau, i.e.,  $|\rho - \rho_c| = 0.33$  or 0.38 for the four study cases. Note that the scaling exponent  $\mu$  cannot be confirmed from the numerical simulations for  $|\rho - \rho_c| \leq 0.03$  due to the statistic nature of  $\rho_c$ , cf. Fig. 5.

According to Eq. (23), the exponent  $\mu$  can be calculated as  $-0.924$  for constant length and uncorrelated networks ( $D_c = 2.0$ ). From the figure, the regression result for  $\mu$  for this case is  $-0.922$ , rather near to the theoretical value. The  $\mu$  exponents are, respectively,  $-1.122$ ,  $-1.257$  and  $-0.919$  for  $D_c = 1.75$  (constant length),  $D_c = 1.62$  (constant length) and  $D_c = 2.0$  (lognormal length). Compared to the predicted  $\mu$  values in Table 3, these regressed  $\mu$  values are rather consistent with the predicted values, confirming the pertinence of the scaling law in Eq. (23). It is to note that the scaling exponent for permeability was estimated as  $\mu = 1.6$  in Mourzenko et al. (2004),  $\mu = 0.4602$  in Jafari and Babadagli (2013) and  $\mu = 1.1$  in Yazdi et al. (2011). The difference is due to the fact that these results neglected the contribution of nonpercolating clusters in networks and the simulation ranges of  $\rho$  were all above the percolation threshold.

### 4.4 Role of Opening Aperture $b$

To investigate the influence of opening aperture  $b$  on the effective permeability or  $K_0$  in Eq. (23), the effective permeability is solved for different crack opening apertures ( $b = 0.001 \sim 0.028$ ) for uncorrelated crack networks ( $D_c = 2.0$ ) with constant length and length ratio  $x = 30$ . The crack density ranges between  $[0, \rho_c]$  with 0.05 as increment. Figure 13 illustrates the effective permeability  $K$  in terms of crack density  $\rho$  for different opening aperture  $b$ . A direct observation is that the impact of  $b$  is less important as  $\rho \ll \rho_c$  and the effect of  $b$  becomes significant only as  $\rho \rightarrow \rho_c$ . It is rather reasonable since after percolation the flow path is continuous and the crack opening has direct impact on the flow rate. In



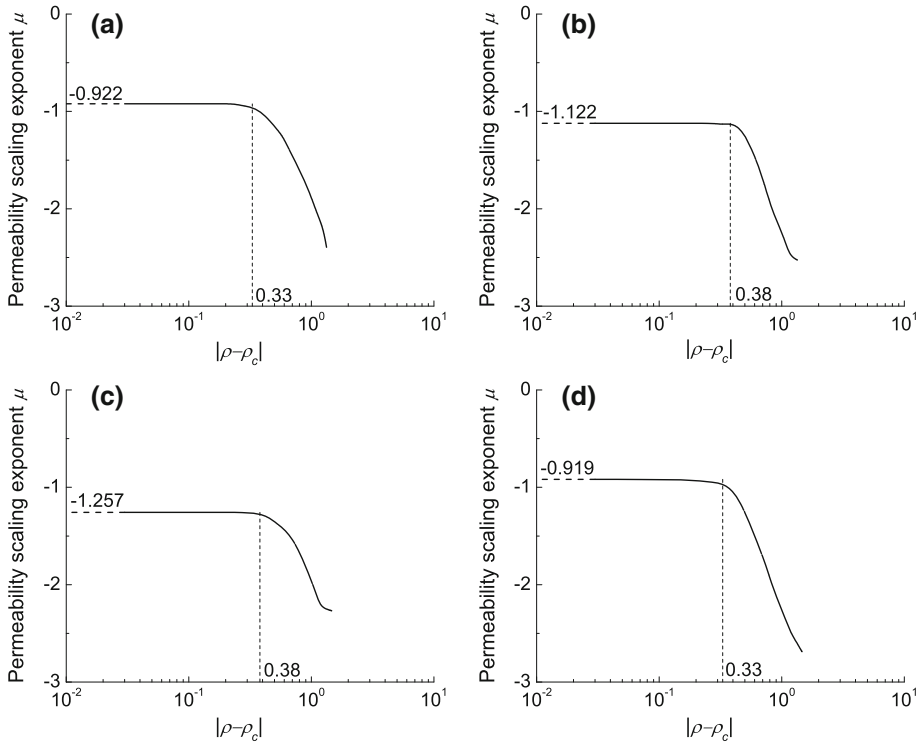


**Fig. 12** Regression of the critical exponent of permeability for  $x = 30$ : **a**  $D_c = 2.0$  and constant length; **b**  $D_c = 1.75$  and constant length; **c**  $D_c = 1.62$  and constant length; **d**  $D_c = 2.0$  and lognormal length

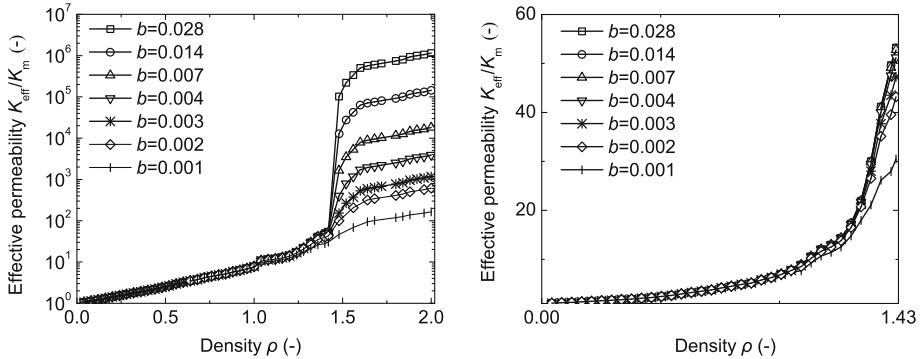


**Fig. 13** Effective permeability  $K_{\text{eff}}$  as a function of density  $\rho$  for various values of  $b$  for constant length randomly oriented case,  $K_m = 10^{-17} \text{ m}^2$ . The density ranging from 0 to  $\rho_c$  is enlarged (right)

other words, the permeability of a percolated network depends strongly on the crack opening aperture.

Figure 14 presents the effective permeability and the term  $K_0$  in terms of crack openings  $b$  for different crack density. The interested density range is  $|\rho - \rho_c| \in [0.03, 0.28]$ , since outside this range for very low values of  $\rho$  the network is not connected, and very large values of  $\rho$  above  $\rho_c$  are out of scope of this research. The results in Fig. 14a show that the

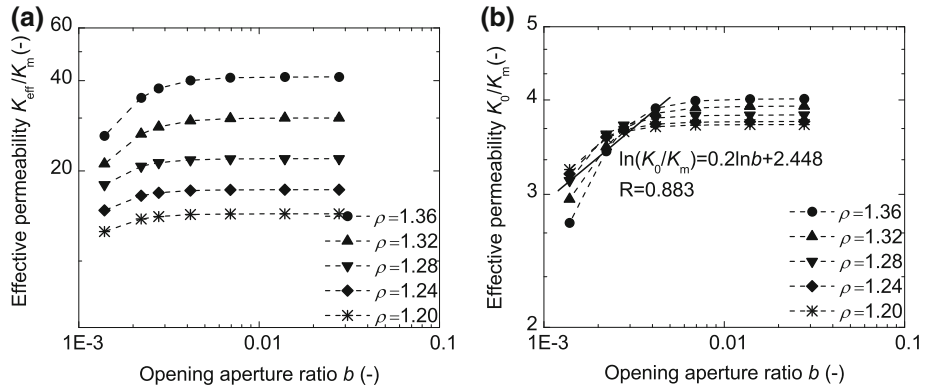


**Fig. 14** Permeability in terms of opening aperture  $b$  for uncorrelated random networks ( $D_c = 2.0$ ), crack density  $\rho = 1.20 \sim 1.36$  and constant crack length: **a** logarithmic plot of  $K_{\text{eff}} \sim b$ ; **b** logarithmic plot of  $K_0 \sim b$

effective permeability  $K_{\text{eff}}$  increases with  $b = 0.001 \sim 0.004$  (corresponding crack opening  $5 \sim 15 \mu\text{m}$ ) for the same density but remains rather stable as  $b$  scales from  $0.007$  to  $0.028$  (corresponding crack opening  $25 \sim 100 \mu\text{m}$ ). This is due to the very high local permeability of cracks with large  $b$ , i.e., the local permeability of crack with opening  $25 \mu\text{m}$  is 7 magnitudes of order higher than  $K_m$ . Figure 14b presents the logarithmic plots of  $K_0/K_m \sim b$  for various values of  $\rho$ . On the logarithmic scale,  $K_0/K_m$  is a linear function of  $b$  for the range  $0.001 \leq b \leq 0.004$ , i.e.,

$$K_0/K_m \propto b^\lambda \quad \text{with } \lambda = 0.2 \quad \text{for } 0.001 \leq b \leq 0.004 \quad (24)$$

and,

$$K = K_0 |\rho - \rho_c|^\mu = 11.57 K_m b^{0.2} |\rho - \rho_c|^{-0.924} \quad (25)$$

This result provides a very useful expression for the effective permeability  $K$  ( $K_m; f, \tau, \rho, b$ ) of the 2D network with cracks of finite apertures. This expression reveals that  $K$  depends on the crack aperture  $b$  via a power law through the term  $K_0$ . Unlike the result in Eq. (7) from Yazdi et al. (2011), the scaling exponent of crack opening  $b$  in Eq. (25) does not depend on the crack density since the contribution of crack density is grouped into the scaling exponent  $\mu$  via connectivity and tortuosity concepts.

### 5 Conclusions

1. This paper investigates the geometry of 2D random crack networks through concepts from continuum percolation theory for a finite domain. The crack density is taken as the basic percolation variable, and the geometry of crack networks is characterized by the percolation threshold ( $\rho_c$ ), scaling exponents ( $\nu, \beta$ ) for percolation probability and correlation length, and the fractal dimension for correlation function ( $D_c$ ). To help the geometry analysis and the later permeability analysis, a new connectivity factor is defined for the 2D random crack networks in finite domain, incorporating the correlation length of crack clusters, domain size and the probability of percolation. This connectivity factor ranges from  $0 \sim 1$  and proved to be consistent with percolation concepts.

2. Numerical samples of crack networks are generated for two different crack length distributions (constant and lognormal) and different crack densities, domain size ratios and clustering degrees. The clustering degree of networks is controlled by the average intersection ratio  $n_{\text{inter}}/N_T$  in the generation of numerical samples, and this clustering degree is well captured by the fractal dimension  $D_c$  of networks. The geometry analysis shows that, for uncorrelated networks ( $D_c = 2.0$ ), the percolation parameters,  $\rho_c$ ,  $\nu$ ,  $\beta$ , do not depend on the crack length distribution and the values from numerical simulations are very near to the theoretical (universal) values reported in the literature while these values will change as the clustering degree of networks increases ( $D_c < 2.0$ ). It is also found that too strong local clustering of cracks will decrease the probability of the global percolation.
3. On the basis of the geometry characterization of 2D random crack networks, the scaling law of the effective permeability of cracked porous solids is established in terms of  $|\rho - \rho_c|$  taking into account the matrix permeability  $K_m$ , crack opening aperture  $b$ , crack connectivity  $f$  and crack tortuosity  $\tau$ . This scaling law is put into the form  $K = K_0(K_m, b)|\rho - \rho_c|^\mu$ , the term  $K_0$  reflects the contribution of porous matrix and crack opening aperture, and the second term reflects the contribution of network geometry through crack density, connectivity and tortuosity. Numerical simulations on effective permeability reveal that the obtained scaling exponent  $\mu$  for uncorrelated networks is very near to theoretical value and the term  $K_0/K_m$  scales with opening aperture  $b$  through a power law. From the simulations in this study,  $|\rho - \rho_c| \in [0.03, 0.28]$  and  $b \in [0.001, 0.004]$ , the scaling exponent for opening aperture is regressed as 0.2.

## References

- Adler, P.M., Thovert, J.F.: Fracture and Fracture Networks. Kluwer, Dordrecht (1999)
- Adler, P.M., Thovert, J.F., Mourzenko, V.V.: Fractured Porous Media. Oxford, London (2013)
- Berkowitz, B.: Analysis of fracture network connectivity using percolation theory. *Math. Geol.* **27**(4), 467–483 (1995)
- Berkowitz, B., Ewing, R.P.: Percolation theory and network modeling applications in soil physics. *Surv. Geophys.* **19**(1), 23–72 (1998)
- Berryman, J.G., Hoversten, G.M.: Modelling electrical conductivity for earth media with macroscopic fluid-filled fractures. *Geophys. Prospect.* **61**(2), 471–493 (2012)
- Bogdanov, I.I., Mourzenko, V.V., Thovert, J.F., Adler, P.M.: Effective permeability of fractured porous media in steady state flow. *Water Resour. Res.* **39**(1), 1023 (2003)
- Bonnet, E., Bour, O., Odling, N.E., Davy, P., Main, I., Cowie, P., Berkowitz, B.: Scaling of fracture systems in geological media. *Rev. Geophys.* **39**(3), 347–383 (2001)
- Bour, O., Davy, P.: Connectivity of random fault networks following a power law fault length distribution. *Water Resour. Res.* **33**(7), 1567–1583 (1997)
- Darcel, C., Bour, O., Davy, P., de Dreuzy, J.R.: Connectivity properties of two-dimensional fracture networks with stochastic fractal correlation. *Water Resour. Res.* **39**(10), 1272 (2003)
- Davy, P., Sornette, A., Sornette, D.: Some consequences of a proposed fractal nature of continental faulting. *Nature* **348**(6296), 56–58 (1990)
- de Dreuzy, J.R., Davy, P., Bour, O.: Hydraulic properties of two-dimensional random fracture networks following a power law length distribution: 1. Effective connectivity. *Water Resour. Res.* **37**(8), 2065–2078 (2001a)
- de Dreuzy, J.R., Davy, P., Bour, O.: Hydraulic properties of two-dimensional random fracture networks following a power law length distribution: 2. Permeability of networks based on lognormal distribution of apertures. *Water Resour. Res.* **37**(8), 2079–2095 (2001b)
- de Dreuzy, J.R., Davy, P., Bour, O.: Hydraulic properties of two-dimensional random fracture networks following power law distributions of length and aperture. *Water Resour. Res.* **38**(12), 1276 (2002)
- Desbarats, A.J.: Spatial averaging of hydraulic conductivity in three-dimensional heterogeneous porous media. *Math. Geol.* **24**(3), 249–267 (1992)

- Guéguen, Y., Dienes, J.: Transport properties of rocks from statistics and percolation. *Math. Geol.* **21**(1), 1–13 (1989)
- Guéguen, Y., Chelidze, T., Le Ravalec, M.: Microstructures, percolation thresholds, and rock physical properties. *Tectonophysics* **279**(1), 23–35 (1997)
- Halperin, B.I., Feng, S., Sen, P.N.: Differences between lattice and continuum percolation transport exponents. *Phys. Rev. Lett.* **54**(22), 2391 (1985)
- Hearn, N.: Effect of shrinkage and load-induced cracking on water permeability of concrete. *ACI Mater. J.* **96**, 234–241 (1999)
- Hestir, K., Long, J.: Analytical expressions for the permeability of random two-dimensional Poisson fracture networks based on regular lattice percolation and equivalent media theories. *J. Geophys. Res.* **95**(B13), 21565–21581 (1990)
- Hunt, A., Ewing, R.: *Percolation Theory for Flow in Porous Media*. Springer, Berlin (2009)
- Jafari, A., Babadagli, T.: Relationship between percolation-fractal properties and permeability of 2-D fracture networks. *Int. J. Rock Mech. Min. Sci.* **60**, 353–362 (2013)
- Kachanov, M.: Effective elastic properties of cracked solids: critical review of some basic concepts. *Appl. Mech. Rev.* **45**(8), 304–335 (1992)
- Lee, Y., Andrade Jr, J.S., Buldyrev, S.V., Dokholyan, N.V., Havlin, S., King, P.R., Paul, G., Stanley, H.E.: Traveling time and traveling length in critical percolation clusters. *Phys. Rev. E* **60**(3), 3425–3428 (1999)
- Lespinasse, M., Désindes, L., Fratzczak, P., Petrov, V.: Microfissural mapping of natural cracks in rocks: implications for fluid transfers quantification in the crust. *Chem. Geol.* **223**(1–3), 170–178 (2005)
- Leung, C.T.O., Zimmerman, R.W.: Estimating the hydraulic conductivity of two-dimensional fracture networks using network geometric properties. *Transp. Porous Media.* **93**(3), 777–797 (2012)
- Li, J.H., Zhang, L.M.: Connectivity of a network of random discontinuities. *Comput. Geotech.* **38**(2), 217–226 (2011)
- Loosveldt, H., Lafhaj, Z., Skoczylas, F.: Experimental study of gas and liquid permeability of a mortar. *Cem. Concr. Res.* **32**(9), 1357–1363 (2002)
- Mandelbrot, B.B.: *The fractal geometry of nature*. W. H. Freeman, New York (1983)
- Masihi, M., King, P.R.: A correlated fracture network: modeling and percolation properties. *Water Resour. Res.* **43**(7), W07439 (2007)
- Mourzenko, V.V., Thovert, J.F., Adler, P.M.: Macroscopic permeability of three-dimensional fracture networks with power-law size distribution. *Phys. Rev. E.* **69**(6), 066307 (2004)
- Norris, A.N.: A differential scheme for the effective moduli of composites. *Mech. Mater.* **4**(1), 1–16 (1985)
- Pan, J.B., Lee, C.C., Lee, C.H., Yeh, H.F., Lin, H.I.: Application of fracture network model with crack permeability tensor on flow and transport in fractured rock. *Eng. Geol.* **116**(1–2), 166–177 (2010)
- Pouya, A., Ghabezloo, S.: Flow around a crack in a porous matrix and related problems. *Transp. Porous Media.* **84**(2), 511–532 (2010)
- Robinson, P.C.: Numerical calculations of critical densities for lines and planes. *J. Phys. A* **17**(14), 2823–2830 (1984)
- Sadeghnejad, S., Masihi, M., King, P.R.: Dependency of percolation critical exponents on the exponent of power law size distribution. *Phys. A* **392**(24), 6189–6197 (2013)
- Samaha, H.R., Hover, K.C.: Influence of microcracking on the mass transport properties. *ACI Mater. J.* **89**, 416–424 (1992)
- Shafiro, B., Kachanov, M.: Anisotropic effective conductivity of materials with nonrandomly oriented inclusions of diverse ellipsoidal shapes. *J. Appl. Phys.* **87**(12), 8561–8569 (2000)
- Sheppard, A.P., Knackstedt, M.A., Pinczewski, W.V., Sahimi, M.: Invasion percolation: new algorithms and universality classes. *J. Phys. A* **32**(49), L521–L529 (1999)
- Somette, D.: Critical transport and failure in continuum crack percolation. *J. Phys.* **49**(8), 1365–1377 (1988)
- Stauffer, D.: Scaling theory of percolation clusters. *Phys. Rep.* **54**(1), 1–74 (1979)
- Stauffer, D., Aharony, A.: *Introduction to Percolation Theory*. Taylor & Francis, London (2003)
- Suzuki, K., Oda, M., Yamazaki, M., Kuwahara, T.: Permeability changes in granite with crack growth during immersion in hot water. *Int. J. Rock Mech. Min. Sci.* **35**(7), 907–921 (1998)
- Torquato, S.: Random heterogeneous media: microstructure and improved bounds on effective properties. *Appl. Mech. Rev.* **44**(2), 37–76 (1991)
- Wilke, S., Guyon, E., de Marsily, G.: Water penetration through fractured rocks: test of a tridimensional percolation description. *J. Int. Assoc. Math. Geol.* **17**(1), 17–27 (1985)
- Wong, P., Koplik, J., Tomanic, J.P.: Conductivity and permeability of rocks. *Phys. Rev. B* **30**(11), 6606–6614 (1984)
- Yazdi, A., Hamzehpour, H., Sahimi, M.: Permeability, porosity, and percolation properties of two-dimensional disordered fracture networks. *Phys. Rev. E* **84**(4), 046317 (2011)

- Zheng, Q.S., Du, D.X.: An explicit and universally applicable estimate for the effective properties of multiphase composites which accounts for inclusion distribution. *J. Mech. Phys. Solids* **49**(11), 2765–2788 (2001)
- Zhou, C., Li, K., Pang, X.: Effect of crack density and connectivity on the permeability of microcracked solids. *Mech. Mater.* **43**(12), 969–978 (2011)
- Zhou, C., Li, K., Pang, X.: Geometry of crack network and its impact on transport properties of concrete. *Cem. Concr. Res.* **42**(9), 1261–1272 (2012)